European Journal of Medicinal Chemistry 60 (2013) 101–111

Contents lists available at SciVerse ScienceDirect

European Journal of Medicinal Chemistry

journal homepage: http://www.elsevier.com/locate/ejmech

Original article

An unprecedented reversible mode of action of β-lactams for the inhibition of human fatty acid amide hydrolase (*h*FAAH)

Marion Feledziak [a,b], Catherine Michaux [c], Didier M. Lambert [b], Jacqueline Marchand-Brynaert [a,*]

[a] *Laboratoire de Chimie Organique et Médicinale, Institute of Condensed Matter and Nanosciences (IMCN), Université catholique de Louvain (UCL), Bâtiment Lavoisier, Place Louis Pasteur L4.01.02, B-1348 Louvain-La-Neuve, Belgium*

[b] *Unité de Chimie Pharmaceutique et de Radiopharmacie, Louvain Drug Research Institute (LDRI), Université catholique de Louvain (UCL), Avenue E. Mounier 73.40, B-1200 Bruxelles, Belgium*

[c] *Unité de Chimie Physique Théorique et Structurale, Facultés Universitaires Notre Dame de la Paix (FUNDP), Rue de Bruxelles 61, B-5000 Namur, Belgium*

ARTICLE INFO

Article history:
Received 20 August 2012
Received in revised form
21 November 2012
Accepted 23 November 2012
Available online 29 November 2012

Keywords:
β-Lactam
Azetidinone
Reversible inhibition
Noncovalent inhibition
Fatty acid amide hydrolase
Serine hydrolase
Endocannabinoid system
Anandamide

ABSTRACT

A series of compound was prepared to clarify the reversible mechanism of β-lactamic hFAAH inhibitors on the one hand, and to modulate some of their physicochemical parameters on the other hand. In particular, two compounds (**4b** and **4e**) were designed to display a potential good leaving group on the crucial carbonyl with a view to possibly acylating the active serine of the hFAAH catalytic triad. Reversibility studies showed that these two compounds retain the reversible mode of inhibition, suggesting a noncovalent interaction between our β-lactams and hFAAH. Finally, pharmacological evaluations of bioisosteres of the lead compound (**4a**, $IC_{50} = 5.3$ nM) revealed that log *P* values and PSA could be optimized without altering the FAAH inhibition (IC_{50} values from 3.65 nM to 70.9 nM).

1. Introduction

Over the last ten years, the selective inhibition of FAAH is one of the most extensive research fields in the world of endocannabinoids [1–6]. Different kinds of electrophilic functions have been broadly studied in view of designing pharmacophores such as α-keto-oxazole (**1**, Chart 1) [7], carbamate (**2**, Chart 1) [8] and urea (**3**, Chart 1) [9]. Structure–activity relationship (SAR) studies performed on a large number of published lead compounds allowed improvements in activity and selectivity of FAAH inhibitors. Moreover, *in vitro* and/or *in vivo* assays confirmed their potential therapeutic interest. FAAH inhibitors were demonstrated to increase the level of anandamide, an endogenous ligand of cannabinoid receptors CB_1 and CB_2, by blocking its FAAH-catalyzed degradation [8,10–13]. Rising the amount of anandamide leads to prolonged beneficial physiological effects due to activation of the cannabinoid receptors. In contrast, it was demonstrated that the cannabinoid receptors activation by exogenous ligand, *e.g.* cannabinoids like Δ^9-THC (tetrahydrocannabinol) or synthetic agonists, maximizes the side effects arising from central nervous system disturbance [14,15]. This is why, taking advantage of the endocannabinoid system, FAAH inhibitors are presently in development for treating inflammation [16,17] and pain [18–20], sleep disorders [21] and CNS diseases [22]. Recently, some clinical trials were achieved with the best representatives of some families, notably PF-04457845 (**3b**) [23]. This compound is involved in a phase II study aimed to collect pharmacodynamic, pharmacokinetic and toxicity data, on the one hand and to evaluate its analgesic efficiency in knee osteoarthritis and its effect on sleep, on the other hand.

Our recent results prompt us to continue investigations about β-lactamic derivatives for FAAH inhibition. Indeed, we have described

Abbreviations: SAR, structure–activity relationship; LC, liquid chromatography; MS, mass spectrometry; *h*FAAH, human fatty acid amide hydrolase; hMAGL, human monoacylglycerol lipase; CB_1, cannabinoid receptor subtype-1; CB_2, cannabinoid receptor subtype-2; AEA, anandamide; 2-AG, 2-arachidonoylglycerol; 2-OG, 2-oleoylglycerol; CNS, central nervous system; PSA, polar surface area; TBDMS, *tert*-butyldimethylsilyl; THF, tetrahydrofuran; DCM, dichloromethane; DMF, dimethylformamide; ACN, acetonitrile; DMSO, dimethyl sulfoxide; DCC, dicyclohexylcarbodiimide; DMAP, dimethylaminopyridine; HMDS, hexamethyldisilazane.

* Corresponding author. Tel.: +32 10 47 27 40; fax: +32 10 47 41 68.
E-mail address: jacqueline.marchand@uclouvain.be (J. Marchand-Brynaert).

0223-5234/$ – see front matter © 2012 Elsevier Masson SAS. All rights reserved.
http://dx.doi.org/10.1016/j.ejmech.2012.11.035

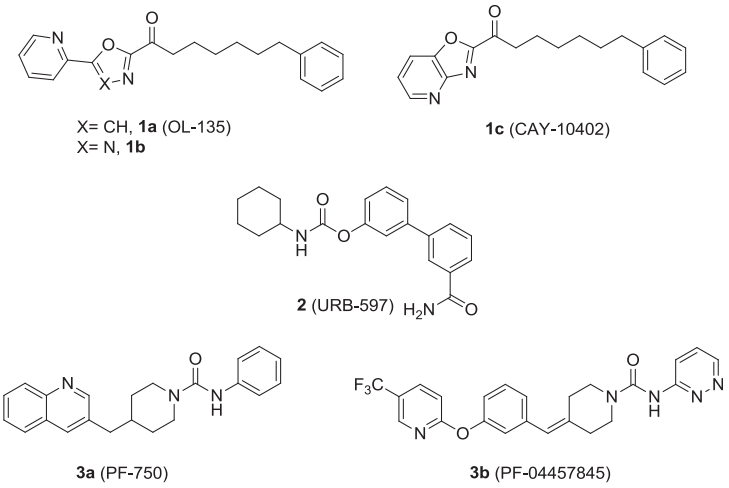

Chart 1. Most studied FAAH inhibitors (Covalent inhibitors).

a new class of inhibitors based on the azetidin-2-one (*i.e.* β-lactam) template and disclosed the lead compound **4a** (*i.e.* 1-(pent-4-enoyl)-3(*S*)-[1(*R*)-(4-phenylbutanoyloxy)-ethyl]-azetidin-2-one, Chart 2) which exhibits a nanomolar activity, and an unusual competitive, fully reversible mode of action [24]. From SAR studies and LC/HRMS analyses, we could establish that the exocyclic carbonyl of the imide function is more essential for the inhibition than the β-lactam carbonyl, and we could exclude that the reversibility of inhibition results from the processing of our inhibitors by FAAH [25]. Thus, β-lactamic inhibitors such as **4a** are not slow substrates of FAAH; they are remaining unchanged in the test solutions. To further explore the reversible mode of inhibition, we designed new compounds based on bioisosteric modifications (**4b**–**4e**, Chart 2). With the aim of modulating the log *P* and polar surface area (PSA) values, two parameters related to solubility and permeability respectively, we synthesized a small library of analogues of **4a**. For that purpose, heteroatoms were inserted in our lead structure **4a** (Chart 2). Because of the great importance of the exocyclic carbonyl of the imide function, carbamate (**4b**), urea (**4c**) and thiourea (**4d**) functions were investigated. These modifications may cause several effects considering lipophilicity, conformational arrangement and the potential occurrence of hydrogen bonds. In addition, they also may change the chemical reactivity and therefore the mode of inhibition. Indeed, compound **4b** for instance, presents a potential leaving group on the exocyclic carbonyl. In the case of a nucleophilic attack of the active serine onto the exocyclic carbonyl, this feature could drive to the formation of a stable acyl-enzyme intermediate, by releasing the allylic alcohol moiety. Thus, we will be able to conclude whether our inhibitors are covalently bound to FAAH via the exocyclic carbonyl – in the case of an irreversible inhibition – or not – in the case of a still reversible inhibition. To further develop this idea of possibly transforming a reversible inhibitor into an irreversible one, an additional compound was designed (**4e**, Chart 2) which presents a better leaving group than **4b** and can be easily prepared from a commercial reagent (namely propyl chlorothioformate).

Finally, to complete the SAR study, the ester side-chain was also modified by introducing heteroatoms at various positions (**5**–**7**, Chart 3).

The effects of all these structural modifications on FAAH inhibition were evaluated *in vitro*, in a competitive hydrolytic assay on human FAAH, and in reversibility assays to evaluate not only the activity but also the mode of inhibition. The selectivity for FAAH versus MAGL was also examined.

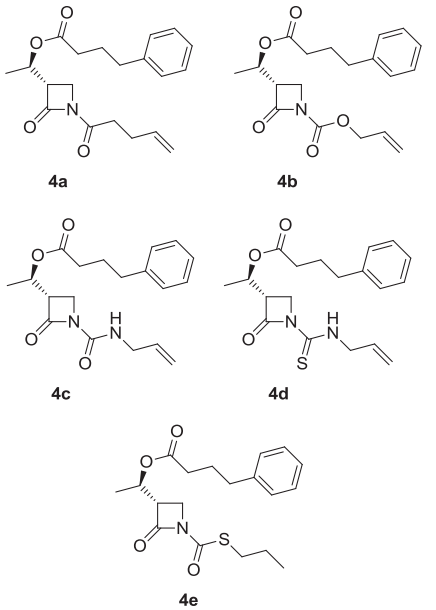

Chart 2. Bioisosteric structures of the imide function.

2. Results

2.1. Chemistry

Compounds synthesis started with precursor **8**, described in our previous publication, which is obtained in two steps from commercially available (3*R*,4*R*)-4-acetoxy-3-[(*R*)-1-(tert-butyldimethylsilyloxy)ethyl]azetidin-2-one. We established a three-step sequence to prepare our library: i) *N*-functionalization, ii) deprotection of silyl ether and iii) *O*-functionalization. Compounds **9a**–**e**

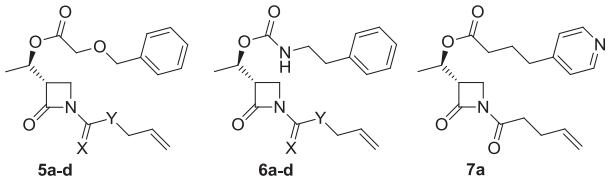

Chart 3. Bioisosteric structures of the ester chain.

were obtained by a *N*-acylation step adapted to the nature of each chain (Scheme 1). Compound **9a** was prepared using 4-pentenoyl chloride in the presence of pyridine in refluxing DCM (80%) while **9b**–**e** were obtained by reaction with allyl chloroformate (**9b**, 82%), allyl isocyanate (**9c**, 57%), allyl isothiocyanate (**9d**, 79%) and propyl chlorothioformate (**9e**, 49%), after deprotonation of **8** in the presence of LiHMDS in THF at −78 °C. Silyl ether protection was removed in acidic conditions leading to compounds **10a**–**e** in moderate to good yields (45–89%, Scheme 1).

The resulting alcohols were engaged in the last step to give the final compounds (Scheme 2). On the one hand, each alcohol (**10a**–**e**) was esterified by one or two usual methods of esterification: i) **4b** (63%), **4c** (88%), **4d** (89%) and **4e** (76%) were synthesized in the presence of pyridine with 4-phenylbutanoyl chloride at room temperature; ii) **5a**–**d** and **7a** were obtained by using 2-(benzyloxy)acetic acid or 4-(pyridin-4-yl)butanoic acid in the presence of dicyclohexylcarbodiimide (DCC) and dimethylaminopyridine (DMAP) in good yields (**5a** (89%), **5b** (58%), **5c** (93%), **5d** (74%), **7a** (64%), Scheme 2). On the other hand, compounds **10a**–**d** were functionalized with phenethyl isocyanate using very mild conditions. Indeed, the conversion into the corresponding alkoxide was not possible and any basic conditions could not be used because of the acidity of H-3 proton. This property drove to a rearrangement which gave *in fine* compound **11** (Scheme 3) by an elimination step followed by azetidinone ring opening. Thus, the carbamate bond was created in the presence of $Ti(OtBu)_4$ as a Lewis acid which catalyzed the nucleophilic attack of the hydroxyl function upon the isocyanate carbonyl function [26]. By this method, compounds were obtained with good yields, in 1 h at room temperature (**6a** (81%), **6b** (64%), **6c** (70%), **6d** (84%), Scheme 2).

All the novel β-lactam derivatives were characterized by the usual spectroscopies; representative ^1H and ^{13}C NMR spectra are provided in the Supporting information. Compounds **4a**–**e**, **5a**–**d**, **6a**–**d** and **7a** are soluble in dichloromethane, tetrahydrofuran, ethyl acetate, acetonitrile, chloroform, acetone, methanol, dimethylformamide and dimethyl sulfoxide (DMSO). They are soluble in aqueous media (Tris–EDTA or phosphate buffers, pH 7.2–7.4) with 5% DMSO.

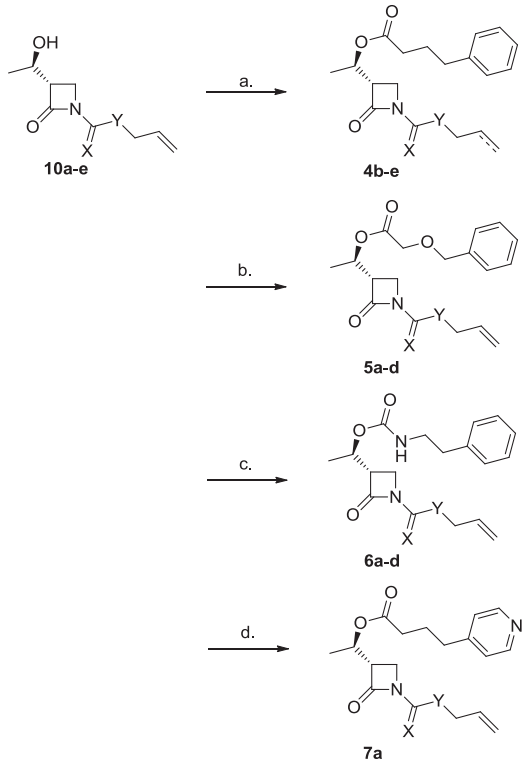

Scheme 2. Reagents and conditions: (a) 4-phenylbutanoyl chloride, pyridine, DCM, rt, 15 h; (b) 2-(benzyloxy)acetic acid, DCC, DMAP, DCM, rt, 15 h; (c) phenethyl isocyanate, $Ti(OtBu)_4$, DCM, rt, 1 h, (d) 4-(pyridin-4-yl)butanoic acid, DCC, DMAP, DCM, rt, 15 h.

2.2. Pharmacology

The library of compounds was tested for FAAH inhibition using human recombinant FAAH as source of enzyme. Some of them were also evaluated as potential MAGL inhibitors to check the selectivity and to study the effect of the exocyclic C=S function of compounds **4**–**6d**. Indeed, MAGL is a serine hydrolase involving three cysteine residues in its active site. According to the HSAB (hard and soft acids and bases) theory, a privileged interaction could occur between the C=S (electrophile) and SH (nucleophile) functions. In addition, the inhibition mode was investigated in the case of two compounds (**4b** and **4e**, Chart 2) which present a potential good leaving group. All the collected results were analyzed taking the relative log *P* and PSA calculated values in consideration (Table 1).

2.2.1. hFAAH inhibition

Human recombinant enzyme, developed in our laboratory [27], was used in a competitive hydrolytic assay using [^{3}H]-AEA as substrate. Tested compounds, enzyme and [^{3}H]-AEA were incubated at 37 °C during 10 min. The extent of inhibition was evaluated by liquid scintillation counting of [^{3}H]-ethanolamine resulting from the hydrolysis of labelled AEA. Considering the results summarized in Table 1, it appeared clearly that the insertion of a sulfur atom (thiocarbonyl) replacing the exocyclic oxygen atom of the imide function, leads to a loss of activity compared to the corresponding bioisosteres (**4d** compared to **4a**–**c**, **5d** to **5a**–**c** and **6d** to **6a**–**c**, IC_{50} = 145.8, 1042 and 959 nM, respectively). This structural moiety suspected to interact with the active serine, is thus less active as a thiocarbonyl function. Comparatively to our previous hit (**4a**, IC_{50} = 5.32 nM, Table 1 and Chart 2), the other bioisosteres were also active in the nanomolar range. They appeared to be good to excellent inhibitors of FAAH, from 70.9 nM (**5c**) to 3.65 nM (**4b**), except **7a**, which exhibited a moderate activity (IC_{50} = 310.1 nM).

Insertion of heteroatoms results in fluctuations of the log *P* values: increased ones with sulfur atoms (notably **4d** and **4e**, 3.47

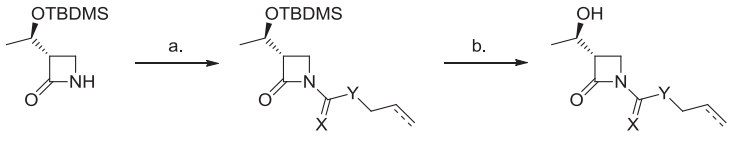

8 **9a**, X= O, Y= CH_2; **b**, X= O, Y= O; **c**, X= O, Y= NH; **d**, X= S, Y= NH; **e**, X=O, Y= S **10a-e**

Scheme 1. Reagents and conditions: (a) 4-pentenoyl chloride, pyridine, DCM, 45 °C, 24 h or allyl chloroformate, allyl isocyanate, allyl isothiocyanate or propyl chlorothioformate, LiHMDS, THF, −78 °C, 4 h; (b) HCl, AcOH, ACN, 0 °C, 3 h.

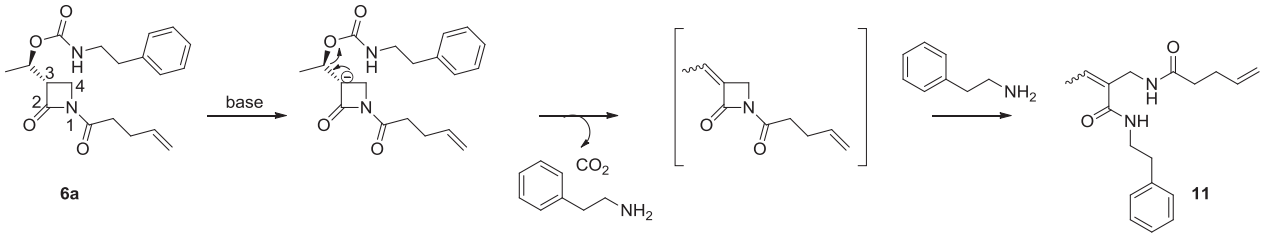

Scheme 3. Proposed mechanism for the formation of **11** (see Supporting information).

and 4.11, respectively) and equalled (**4b**, 3.31) or lowered ones with nitrogen or oxygen atoms (from 2.65 to 1.41, **6d** and **5c**, respectively). We could not correlate inhibitory potency and log *P* values but we could observe that fluctuations in the lipophilicity of some compounds did not really alter their activity compared to **4a**: for instance, **4c** presents a similar activity with a lower log *P* value (IC_{50} = 5.32 and 5.56 nM, and log *P* = 3.25 and 2.59, respectively); **5a**–**b** and **6a**–**c** differ by a log *P* decrease of one logarithmic unit at least and retain excellent activities (*e.g.* **6c**, IC_{50} = 28.6 nM and log *P* = 1.76) and finally, compound **5c** displays the lowest log *P* value and a good activity (IC_{50} = 70.9 nM and log *P* = 1.41). Inversely to log *P* values, PSAs tend to increase with heteroatoms insertion. But, alike log *P* fluctuations, no direct correlation could be done. We observed good to excellent activities for different modulations of PSA.

2.2.2. hMAGL inhibition

Human recombinant enzyme, developed in our laboratory [29], was used in a competitive hydrolytic assay using [^{3}H]-2-OG as substrate. Tested compounds, enzyme and [^{3}H]-2-OG were pre-incubated at room temperature during 30 min and incubated at 37 °C during 10 min. The extent of inhibition was evaluated by liquid scintillation counting of [^{3}H]-glycerol resulting from the hydrolysis of labelled 2-OG. All the tested compounds presented a very low activity, those with a thiocarbonyl function (**4**–**6d**) and the other ones (**4b**, **4c** and **5c**). IC_{50} values ranged from 10.3 μM (**4b**) to 121.7 μM (**5d**) and compounds **4d** and **6d** inhibited 60% and 25% of MAGL at 10^{-3} M, respectively. Comparatively to the lead compound (**4a**), there is a high selectivity for the inhibition of FAAH: for instance, compounds **4b** and **4c** are respectively 2800 and 18,000 times more potent against FAAH.

Table 1
Determination of inhibitory potential on hFAAH and hMAGL, log *P* and PSA parameters.

Compound	log *P*[a]	PSA[a,b]	pI50 (hFAAH)	IC_{50}[c] on hFAAH	IC_{50}[c] on hMAGL
4a	3.25	76.57	−8.27 ± 0.05	5.32	4060
4b	3.31	72.91	−8.44 ± 0.03	3.65	10,300
4c	2.59	75.71	−8.26 ± 0.03	5.56	98,410
4d	3.47	90.73	−6.84 ± 0.03	145.8	60% inh at 10^{-3} M
4e	4.11	88.98	−7.92 ± 0.07	12.1	18,960
5a	2.08	72.91	−7.51 ± 0.02	30.9	nd
5b	2.14	82.14	−7.52 ± 0.06	30.1	nd
5c	1.41	84.94	−7.15 ± 0.02	70.9	56,850
5d	2.30	99.96	−5.98 ± 0.02	1042	121,700
6a	2.43	75.71	−7.48 ± 0.03	33.2	nd
6b	2.49	84.94	−7.92 ± 0.02	12.1	nd
6c	1.76	87.74	−7.54 ± 0.02	28.6	nd
6d	2.65	102.76	−6.02 ± 0.05	959	25% inh at 10^{-3} M
7a	2.03	76.57	−6.51 ± 0.02	310.1	nd

[a] Calculated via Marvinsketch.
[b] Calculated by the atom-based method (topological PSA or TPSA) of Ertl, Rohde and Seltzer [28]. It consists in the summation of tabulated values corresponding to commonly used polar fragments (N and O) and slightly less one (S).
[c] In nM, from three independent experiments.

2.2.3. Mode of inhibition

To address the reversibility question, we selected two inhibitors featuring good leaving-groups near the exocyclic carbonyl (**4b** and **4e**, Chart 2). Wash-out experiments were undertaken to measure the recovery of enzyme activity after a rapid and large dilution of the inhibitor–enzyme mixtures. Results were collected after 0, 30 and 90 min.

The enzyme activity should be almost totally recovered if the inhibitor is reversible, but the enzyme should remain largely inhibited in the case of an irreversible inhibition. Here, the rapid and large dilution led to the recovery of activity for **4b** and **4e**, similarly to **1c** (CAY-10402, Chart 1) [30]. As a further control we used two known irreversible FAAH inhibitors, **2** [31] (URB-597, Chart 1) and **3a** (PF-750, Chart 1) [32]; we found that the enzyme activity is still largely inhibited after the dilution experiment (Fig. 1).

2.2.4. Docking studies

Recent publications have shown the different binding modes of inhibitors into the FAAH active site thanks to the X-ray diffraction analysis of co-crystals obtained from an engineered humanized rat FAAH (*h*/*r*FAAH). Molecules **2** (URB-597, Chart 1) [33] and **3a** (PF-750, Chart 1) [12] are trapped as stable acyl-enzyme intermediates after expelling their respective leaving-group. Molecule **1a** (OL-135, Chart 1) is quenched as the tetrahedral intermediate [19,34,35]. Interestingly, noncovalent and covalent states of the same inhibitor **1b** (Chart 1) into *h*/*r*FAAH could be observed: the catalytic residues Ser241, Ser217 and Lys142 occupy essentially identical positions in both complexes [36]. A noncovalent complex between the reversible inhibitor **12** (Chart 4) and *r*FAAH was also disclosed [37,38].

The *h*FAAH enzyme we used is not yet crystallized. In order to bring out a potential binding mode of the present inhibitors in

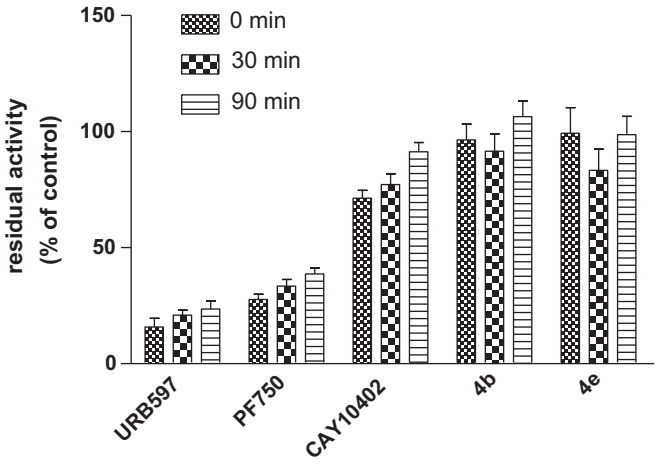

Fig. 1. Test of reversibility: influence of a rapid and large dilution on the recovery of hFAAH activity (studies after 0, 30 and 90 min following the rapid and large dilution).

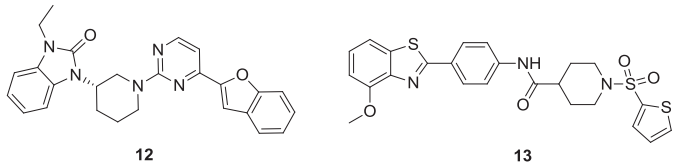

12 13

Chart 4. Noncovalent inhibitors of FAAH.

*h*FAAH, docking studies were performed in the catalytic site of the enzyme, inspired by the *h*/*r*FAAH crystallographic data [36]. This active pocket is formed by a hydrophobic tunnel, called the acyl chain binding channel (ACB), leading from the membrane-bound surface to the hydrophilic catalytic triad (Ser241, Ser217, and Lys142). A second tunnel, the cytoplasmic access channel (CA), is exposed to the solvent. A third channel composed of three phenylalanine residues (Phe388, Phe381, and Phe192), called the "phenyl pocket", lies close to the ACB channel. We docked the compounds into the crystal structure of the humanized rat FAAH as the Michaelis complexes. The emerging binding mode, pictured here for **4b**, **4c** and **4e**, is the same as the one previously described for **4a** (Fig. 3) [24]. The phenyl chain lies in the "phenyl pocket" and interacts with the three phenylalanines Phe192, Phe381, and Phe388. The catalytic serine Ser241 is close to the lactam and imide carbonyls. The alkene chain lies at the beginning of ACB channel. Hydrogen bonds are observed between Ser241 and the exocyclic CO, between Thr236 and the lactam CO, between the ester CO and the NH group of Val270 and Cys269.

3. Discussion and conclusion

The competitive, reversible inhibition of our inhibitors appears unique in the β-lactam literature, to the best of our knowledge. Whereas β-lactams are widely known to inhibit traditional serine hydrolases (*i.e.* serine enzymes featuring the Ser-Asp-His catalytic triad) [39] in an irreversible manner (DD-peptidases [40], β-lactamases [41,42], elastases [43–47]), a reversible mechanism occurs between our compounds and hFAAH of which the catalytic pocket involves the unusual Ser-Ser-Lys catalytic triad [48]. We have firmly established that our β-lactams are not processed by the enzyme [25] and that, after rapid and large dilution of enzyme–inhibitor mixtures, the enzyme recovers its full activity.

From our previous studies, we know that the key moiety for interaction with hFAAH is the exocyclic carbonyl group of the imide function [25]. As a matter of fact, the replacement of this carbonyl by a thiocarbonyl led to an important decrease of the inhibition activity (compounds **4d**, **5d** and **6d**). As shown in Fig. 2, the reversible inhibition of hFAAH could result from the formation of a high affinity noncovalent complex between the enzyme and the β-lactamic inhibitor (step 1), eventually leading to a covalent tetrahedral intermediate by nucleophilic attack of the active serine Ser241 on the C=X bond of the inhibitor (step 2). In the absence of good leaving-group on this intermediate (Y is CH_2), the step 2 could be reversible. Such modes of action (*i.e.* steps 1 and 2) have been recently demonstrated with co-crystal structures: reversible covalent interaction with OL-135 (**1a**) and other α-keto-oxazoles [19,34,35] and reversible noncovalent interaction with ketobenzimidazole **12** (Chart 4) [37,38]. We speculated that the presence of a potential leaving group on the tetrahedral intermediate (Y is a heteroatom), could draw the reaction towards the acyl-enzyme intermediate (step 3). Depending on the stability of this intermediate versus hydrolysis, the resulting inhibition could be irreversible or slowly reversible, when the inhibitor behaves as a bad substrate.

Irreversible inhibition of hFAAH, due to the formation of a stable acyl-enzyme intermediate, is the recognized mode of action of URB-597 (**2**, Chart 1) [33,49], PF-04457845 (**3b**, Chart 1) [12,32,50] and related carbamates and ureas. Independently of the presence of a potential leaving group in their structures, our β-lactamic inhibitors act systematically as reversible inhibitors. Our results strongly suggest a similar mode of action as ketobenzimidazole **12** (Chart 4) [38] or benzothiazole **13** (Chart 4) [51], *i.e.* an inhibition due only to the high affinity of our β-lactams with aminoacid residues of the active site (step 1). By docking experiment we can propose a possible binding mode where the enzyme–inhibitor Michaelis complex is stabilized by hydrogen bondings of the exocyclic and β-lactam carbonyls with, respectively, the Ser241 and Thr236 residues of the active site, on the one hand and by hydrophobic interactions of the 4-phenyl-butanoyl chain in the "phenyl pocket", on the other hand (Fig. 3). As a matter of fact, we observed a decrease of activity when the phenyl ring of this ester chain is replaced by a pyridine ring (**7a**). This observation suggests a loss of affinity in the hydrophobic cavity where pyridine, probably protonated, does not stabilize the interaction. All the tested compounds were highly selective for the hFAAH inhibition versus hMAGL. The hypothesis of a favourable interaction between the thiocarbonyl group of β-lactams **4d**, **5d** and **6d** and cysteine residues of the hMAGL catalytic pocket, was not verified.

Finally, we could not correlate log *P* values, PSAs and inhibition potency. Modification of these physicochemical parameters did not seem to influence greatly the inhibition of FAAH. However, we showed that it is possible to improve physicochemical parameters, *i.e.* solubility and permeability factors, without altering the inhibition of hFAAH. Indeed, the best representatives of this study conserved a nanomolar activity against hFAAH with lower log *P* value and PSA. This information is important for candidates selection in view of *in vivo* experiments with β-lactamic hFAAH inhibitors.

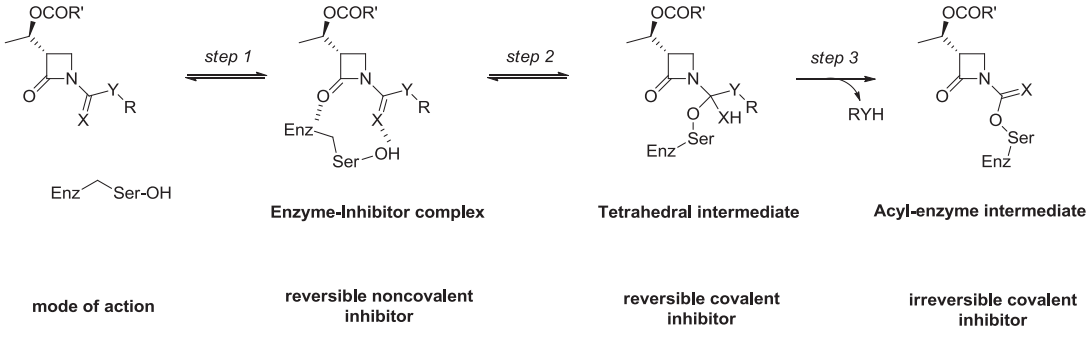

Fig. 2. Possible mechanisms of inhibition (X = O, S; Y = CH_2, NH, O, S).

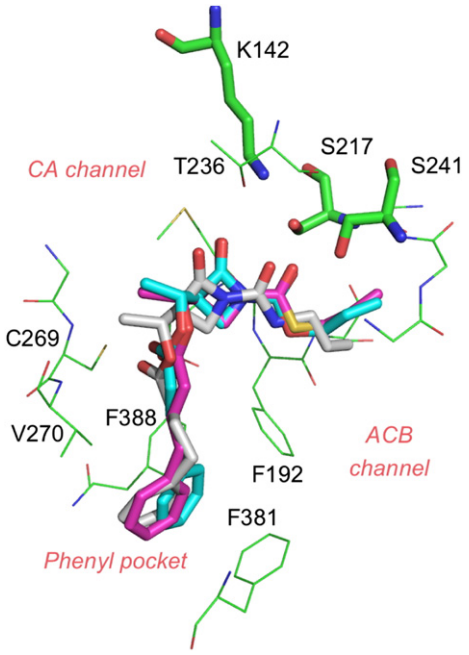

Fig. 3. Proposed binding mode of **4b** (light blue), **4c** (white) and **4e** (magenta) in the active site of the humanized rat FAAH. H atoms were removed for clarity. (For interpretation of the references to colour in this figure legend, the reader is referred to the web version of this article.)

4. Experimental section

4.1. Chemistry

All solvents, including anhydrous solvents, and reagents were purchased from Acros Organics, Alfa Aesar, Cayman chemical, Fluka, Sigma–Aldrich or VWR, and used without purifications. [^{3}H]-AEA (60 Ci/mmol) was purchased from American Radiolabeled Chemical (St Louis, MO). UltimaGold scintillation liquid was bought from Perkin Elmer. All reactions under dry conditions were performed under argon atmosphere in flame-dried glassware. Nuclear Magnetic Resonance (^{1}H NMR and ^{13}C NMR) spectra were recorded at 300 MHz for proton and 75 MHz for carbon (Bruker Avance 300) or 500 MHz for proton and 125 MHz for carbon (Bruker Avance 500) using deuterated chloroform. Chemical shifts are reported in ppm relative to the signals of residual non-deuterated solvent ($CDCl_3$ 7.26 and 77.16 ppm). NMR coupling constants (J) are reported in hertz. Melting points (mp) were determined on a Büchi B-540 apparatus calibrated with caffeine, vanillin and phenacetin. Rotations were recorded on Atago Ap-100 polarimeter, at 25 °C, in $CHCl_3$. Concentrations are given in percentage (g/100 mL). Low resolution mass spectra were acquired using a Thermo Finnigan LCQ spectrometer in negative mode of electrospray ionisation (ESI). High Resolution Mass Spectrometry (HRMS) analyses were performed using a QExactive (Thermo Scientific) spectrometer. Infrared (IR) spectra were recorded using FTIR-8400S Shimadzu apparatus. Products were analyzed as thin films deposited on a Se–Zn crystal by evaporation of CH_2Cl_2 solutions. TLC analysis was performed on Merck silica gel 60F_{254} with detection under UV light, and flash chromatography was performed on silica gel (40–60 mesh) purchased from Rocc (Belgium). Purity of tested compounds was assessed by HPLC on chiralpak IA column (4.6 mm × 250 mm, 5 μm particle size) using hexane/isopropanol eluant (95:5), at a flow rate of 1.0 mL/min and on symmetry C18 column (4.6 mm × 250 mm, 5 μm particle size) using a gradient of acetonitrile/H_2O eluant (50:50 to 100:0), at a flow rate of 1.2 mL/min (purity ≥ 95%).

4.2. General procedure for coupling chloro(thio)formate with amide function (**9b** and **9e**)

To a stirred solution of azetidinone (1 equiv) **8** in dry THF (7 mL/mmol) cooled at −78 °C, was dropwise added a solution of LiHMDS (1.1 equiv) in dry THF (1 M), under argon atmosphere. The mixture was stirred for 30 min at −78 °C and the chloro(thio)formate (1.1 equiv) was added. After 1 h at −78 °C, the solution was allowed to warm up to r.t. and additionally stirred for 1 h. The reaction was quenched, at low temperature, with brine and diluted with DCM. The aqueous layers were extracted with DCM three times. The organic layers were combined, dried over $MgSO_4$, filtered and concentrated under vacuum. After purification by flash chromatography (cyclohexane/AcOEt), colourless oils were obtained (**9b** and **9e**).

4.2.1. 1-(Propyl-3-enoxy)carbonyl-(3S)-3-[(1R)-(tert-butyldimethylsilyloxy)ethyl]azetidin-2-one (**9b**)

Purification by flash chromatography (cyclohexane/AcOEt 5:2) gave **9b** (112 mg, 82%) as a colourless oil: Rf = 0.54 (cyclohexane/AcOEt, 5:3); ^{1}H NMR (500 MHz, $CDCl_3$): δ = 0.02 (s, 3H), 0.04 (s, 3H), 0.81 (s, 9H), 1.15 (d, J = 6.3 Hz, 3H), 3.20 (m, 1H), 3.55 (m, 1H), 3.70 (dd, J = 3.5 Hz, J = 6.5 Hz, 1H), 4.26 (m, 1H), 4.60–4.76 (m, 2H), 5.20–5.38 (m, 2H), 5.84–5.96 ppm (m, 1H); ^{13}C NMR (125 MHz, $CDCl_3$): δ = −5.1, −4.2, 14.2, 17.9, 22.3, 25.7, 39.7, 57.2, 64.8, 66.9, 119.1, 131.5, 149.1, 165.8 ppm; IR: ν = 2852–2976, 1805, 1730, 1375, 1325, 1277, 1259, 839 cm^{-1}; MS (ESI): m/z (%): 314.09 (16) $[M + H]^+$, 336.13 (41) $[M + Na]^+$, 648.93 (100) $[2M + Na]^+$; HRMS-ESI: m/z $[M + H]^+$ calcd for $C_{15}H_{28}NO_4Si$: 314.17821, found: 314.17859.

4.2.2. 1-(Propyl-3-sulfanyl)carbonyl-(3S)-3-[(1R)-(tert-butyldimethylsilyloxy)ethyl]azetidin-2-one (**9e**)

Purification by flash chromatography (cyclohexane/AcOEt 5:1) gave **9e** (71 mg, 49%) as a colourless oil: Rf = 0.63 (cyclohexane/AcOEt, 5:2); ^{1}H NMR (500 MHz, $CDCl_3$): δ = 0.04 (s, 3H), 0.05 (s, 3H), 0.82 (s, 9H), 0.97 (t, J = 7.4 Hz, 3H), 1.17 (d, J = 6.3 Hz, 3H), 1.65 (m, 2H), 2.85–2.99 (m, 2H), 3.23 (m, 1H), 3.61 (m, 1H), 3.75 (dd, J = 3.5 Hz, J = 6.8 Hz, 1H), 4.26–4.33 ppm (m, 1H); ^{13}C NMR (125 MHz, $CDCl_3$): δ = −5.1, −4.2, 13.3, 17.9, 22.3, 23.0, 25.7, 31.1, 40.0, 56.7, 64.7, 165.5, 165.7 ppm; IR: ν = 2856–2949, 1786, 1668, 1306, 1252, 1136, 1076, 1018, 839 cm^{-1}; MS (ESI): m/z (%): 332.17 (60) $[M + H]^+$, 354.15 (89) $[M + Na]^+$, 685.32 (100) $[2M + Na]^+$; HRMS-ESI: m/z $[M + H]^+$ calcd for $C_{15}H_{30}NO_3SSi$: 332.17102, found: 332.17127.

4.3. General procedure for coupling iso(thio)cyanate with amide function (**9c** and **9d**)

To a stirred solution of azetidinone (1 equiv) **8** in dry THF (7 mL/mmol) cooled at −78 °C, was dropwise added a solution of LiHMDS (1.1 equiv) in dry THF (1 M), under argon atmosphere. The mixture was stirred for 30 min at −78 °C and the iso(thio)cyanate (1.1 equiv) was added. After 1 h at −78 °C, the solution was allowed to warm up to r.t. and additionally stirred for 1 h. The reaction was quenched, at low temperature, with brine and diluted with DCM. The aqueous layers were extracted with DCM three times. The organic layers were combined, dried over $MgSO_4$, filtered and concentrated under vacuum. After purification by flash chromatography (cyclohexane/AcOEt), colourless oils were obtained (**9c** and **9d**).

4.3.1. 1-(Propyl-3-enamino)carbonyl-(3S)-3-[(1R)-(tert-butyldimethylsilyloxy)ethyl]azetidin-2-one (**9c**)

Purification by flash chromatography (DCM/AcOEt 98:2) gave **9c** (78 mg, 57%) as a colourless oil: Rf = 0.42 (cyclohexane/AcOEt, 5:3); ^{1}H NMR (500 MHz, $CDCl_3$): δ = −0.04 (s, 3H), −0.02 (s, 3H), 0.75 (s, 9H), 1.10 (d, J = 6.3 Hz, 3H), 3.17 (m, 1H), 3.51 (m, 1H), 3.63 (dd, J = 3.1 Hz, J = 6.3 Hz, 1H), 3.74–3.80 (m, 1H, AB system), 3.82–3.89

(m, 1H, AB system), 4.20 (m, 1H), 5.00–5.13 (m, 2H), 5.74 (m, 1H), 6.52 ppm (br t, J = 5.7 Hz, 1H); ^{13}C NMR (125 MHz, $CDCl_3$): δ = −5.3, −4.3, 17.3, 22.1, 25.5, 38.9, 41.9, 56.5, 64.5, 116.0, 133.9, 150.4, 168.2 ppm; IR: ν = 2856–2957, 1765, 1699, 1531, 1464, 1337, 1259, 1140, 1076, 839 cm^{-1}; MS (ESI): m/z (%): 313.19 (100) $[M + H]^+$, 625.38 (38) $[2M + H]^+$; HRMS-ESI: m/z $[M + H]^+$ calcd for $C_{15}H_{29}N_2O_3Si$: 313.19420, found: 313.19431.

4.3.2. 1-(Propyl-3-enamino)thiocarbonyl-(3S)-3-[(1R)-(tert-butyldimethylsilyloxy)ethyl]-azetidin-2-one (**9d**)

Purification by flash chromatography (cyclohexane/AcOEt 5:1) gave **9d** (113 mg, 79%) as a colourless oil: Rf = 0.69 (chex/AcOEt, 5:3); ^{1}H NMR (500 MHz, $CDCl_3$): δ = 0.01 (s, 3H), 0.03 (s, 3H), 0.79 (s, 9H), 1.17 (d, J = 6.3 Hz, 3H), 3.17 (m, 1H), 3.72 (dd, J = 6.9 Hz, J = 6.0 Hz 1H), 3.84 (dd, J = 3.2 Hz, J = 6.9 Hz, 1H), 4.13–4.21 (m, 1H), 4.23–4.34 (m, 2H), 5.13–5.24 (m, 2H), 5.83 (m, 1H), 8.41 ppm (br s, 1H); ^{13}C NMR (125 MHz, $CDCl_3$): δ = −5.2, −4.1, 17.8, 22.2, 25.6, 42.3, 46.9, 55.1, 64.7, 117.4, 132.2, 166.5, 178.3 ppm; IR: ν = 2858–2953, 1755, 1533, 1342, 1323, 1254, 1140, 1074, 1020, 839 cm^{-1}; MS (ESI): m/z (%): 329.17 (100) $[M + H]^+$, 351.15 (80) $[M + Na]^+$; HRMS-ESI: m/z $[M + H]^+$ calcd for $C_{15}H_{29}N_2O_2SSi$: 329.17135, found: 329.17153.

4.4. General procedure for silyl ether deprotection (**10a–e**)

To a stirred suspension of silyl ether (1 equiv) in acetonitrile (30 mL/mmol) at −5 °C was added dropwise 12 N HCl (5 equiv) and 17 N AcOH (7 equiv). The mixture was stirred for 30 min at −5 °C, and for 3 h at 0 °C. Acetonitrile was removed under vacuum, and the oily residue was diluted in ethyl acetate. The organic layer was washed with 10% $NaHCO_3$ and brine, dried over $MgSO_4$, filtered and concentrated under vacuum. After purification by flash chromatography (ethyl acetate 100%) a white solid (**10c**) or colourless oils (**10b**, **d**–**e**) were obtained.

4.4.1. 1-(Propyl-3-enoxy)carbonyl-(3S)-3-[(1R)-hydroxyethyl] azetidin-2-one (**10b**)

Purification by flash chromatography (AcOEt 100%) gave **10b** (241 mg, 76%) as a colourless oil: Rf = 0.57 (AcOEt 100%); ^{1}H NMR (500 MHz, $CDCl_3$): δ = 1.24 (d, J = 6.4 Hz, 3H), 2.85 (br s, 1H), 3.22–3.31 (m, 1H), 3.60–3.71 (m, 2H), 4.22 (m, 1H), 4.67 (m, 2H), 5.20–5.41 (m, 2H), 5.91 (m, 1H); ^{13}C NMR (125 MHz, $CDCl_3$): δ = 21.5, 40.6, 56.8, 64.6, 67.1, 119.3, 131.3, 149.0, 165.8; IR: ν = 3447, 2912–2988, 1790, 1732, 1379, 1319, 1252, 1128, 1047 cm^{-1}; MS (ESI): m/z (%): 199.98 (2) $[M + H]^+$, 222.10 (16) $[M + Na]^+$, 420.81 (100) $[2M + Na]^+$; HRMS–CI: m/z $[M + H]^+$ calcd for $C_9H_{14}NO_4$: 200.09288, found: 200.09274.

4.4.2. 1-(Propyl-3-enamino)carbonyl-(3S)-3-[(1R)-hydroxyethyl] azetidin-2-one (**10c**)

Purification by flash chromatography (AcOEt 100%) gave **10c** (24 mg, 47%) as a colourless oil: Rf = 0.29 (AcOEt 100%); ^{1}H NMR (500 MHz, $CDCl_3$): δ = 1.27 (d, J = 6.4 Hz, 3H), 2.73 (br s, 1H), 3.28 (m, 1H), 3.65 (m, 2H), 3.82–3.92 (m, 2H), 4.20 (m, 1H), 5.10–5.21 (m, 2H), 5.81 (m, 1H), 6.58 ppm (br s, 1H); ^{13}C NMR (125 MHz, $CDCl_3$): δ = 21.7, 40.0, 42.2, 56.3, 64.7, 116.6, 133.8, 150.6, 168.2 ppm; IR: ν = 3354, 2926–2961, 1755, 1678, 1528, 1331, 1286, 1265, 1138 cm^{-1}; MS (ESI): m/z (%): 199.11 (34) $[M + H]^+$, 221.09 (100) $[M + Na]^+$; HRMS-ESI: m/z $[M + H]^+$ calcd for $C_9H_{15}N_2O_3$: 199.10772, found: 199.10769.

4.4.3. 1-(Propyl-3-enamino)thiocarbonyl-(3S)-3-[(1R)-hydroxyethyl]azetidin-2-one (**10d**)

Purification by flash chromatography (AcOEt 100%) gave **10d** (66 mg, 89%) as a white solid: Rf = 0.26 (cyclohexane/AcOEt 5:3); ^{1}H NMR (500 MHz, $CDCl_3$): δ = 1.30 (d, J = 6.4 Hz, 3H), 2.10 (br s, 1H), 3.25 (m, 1H), 3.82 (m, 2H), 4.20–4.32 (m, 3H), 5.18–5.29 (m, 2H), 5.89 (m, 1H), 8.43 ppm (br s, 1H); ^{13}C NMR (125 MHz, $CDCl_3$): δ = 21.7, 43.1, 47.2, 54.5, 64.8, 117.9, 132.1, 166.1, 178.2 ppm; IR: ν = 2934, 1749, 1539, 1340, 1238, 1134 cm^{-1}; MS (ESI): m/z (%): 215.09 (25) $[M + H]^+$, 237.07 (100) $[M + Na]^+$; HRMS-ESI: m/z $[M + H]^+$ calcd for $C_9H_{15}N_2O_2S$: 215.08487, found: 215.08501.

4.4.4. 1-(Propyl-3-sulfanyl)carbonyl-(3S)-3-[(1R)-hydroxyethyl] azetidin-2-one (**10e**)

Purification by flash chromatography (AcOEt 100%) gave **10e** (21 mg, 45%) as a colourless oil: Rf = 0.21 (cyclohexane/AcOEt 5:3); ^{1}H NMR (500 MHz, $CDCl_3$): δ = 0.98 (t, J = 7.4 Hz, 3H), 1.29 (d, J = 6.4 Hz, 3H), 1.66 (m, 2H), 2.02 (br s, 1H), 2.94 (m, 2H), 3.30 (m, 1H), 3.68–3.73 (m, 2H), 4.26 ppm (m, 1H); ^{13}C NMR (125 MHz, $CDCl_3$): δ = 13.4, 21.7, 23.0, 31.2, 40.9, 56.2, 64.8, 165.2, 165.8 ppm; IR: ν = 2959, 1780, 1664, 1306, 1238, 1130 cm^{-1}; MS (ESI): m/z (%): 218.08 (12) $[M + H]^+$, 240.06 (100) $[M + Na]^+$, 457.14 (75) $[2M + Na]^+$; HRMS-ESI: m/z $[M + H]^+$ calcd for $C_9H_{16}NO_3S$: 218.08454, found: 218.08466.

4.5. General procedure for esterification with acyl chloride (**4b–e**)

To a stirred solution of alcohol precursor (1 equiv) in dry dichloromethane (20 mL/mmol), at 20 °C, were added pyridine (2 equiv) and 4-phenylbutanoyl chloride (2 equiv) under argon atmosphere. After stirring overnight, the mixture was diluted in DCM and the excess of acyl chloride was quenched by 10% aqueous Na_2CO_3. The organic layer was washed with 3 N HCl and brine, dried over $MgSO_4$, filtered and concentrated under vacuum. After purification by flash chromatography (DCM/EtOAc), a colourless oil was obtained in all cases.

4.5.1. 1-(Propyl-3-enoxy)carbonyl-(3S)-3-[(1R)-(4-phenylbutanoyloxy)ethyl]azetidin-2-one (**4b**)

Purification by flash chromatography (DCM/AcOEt 98:2) gave **4b** (44 mg, 63%) as a colourless oil: $[\alpha]_D$ = −0.32 (c = 0.60); Rf = 0.43 (DCM/AcOEt 95:5); ^{1}H NMR (300 MHz, $CDCl_3$): δ = 1.34 (d, J = 6.4 Hz, 3H), 1.92 (m, 2H), 2.31 (m, 2H), 2.62 (m, 2H), 3.40 (m, 1H), 3.59 (dd, J = 3.6 Hz, J = 7.0 Hz, 1H), 3.70 (m, 1H), 4.69 (d, J = 5.7 Hz, 2H), 5.21–5.42 (m, 3H), 5.92 (m, 1H), 7.12–7.32 ppm (m, 5H); ^{13}C NMR (75 MHz, $CDCl_3$): δ = 18.5, 26.5, 33.7, 35.1, 41.4, 54.5, 67.26, 67.34, 119.4, 126.1, 128.5, 128.6, 131.2, 141.3, 149.0, 163.7, 172.5 ppm; IR: ν = 2912–2959, 1805, 1798, 1728, 1454, 1377, 1327, 1186, 1126 cm^{-1}; MS (ESI): m/z (%): 346.04 (3) $[M + H]^+$, 368.19 (100) $[M + Na]^+$; HRMS-ESI: m/z $[M + Na]^+$ calcd for $C_{19}H_{23}NO_5Na$: 368.1474, found: 368.1464.

4.5.2. 1-(Propyl-3-enamino)carbonyl-(3S)-3-[(1R)-(4-phenylbutanoyloxy)ethyl]azetidin-2-one (**4c**)

Purification by flash chromatography (DCM/AcOEt 98:2) gave **4c** (61 mg, 88%) as a colourless oil: $[\alpha]_D$ = −0.12 (c = 0.51); Rf = 0.36 (cyclohexane/AcOEt 5:3); ^{1}H NMR (500 MHz, $CDCl_3$): δ = 1.32 (d, J = 6.4 Hz, 3H), 1.90 (m, 2H), 2.28 (m, 2H), 2.60 (m, 2H), 3.40 (m, 1H), 3.57 (dd, J = 3.2 Hz, J = 6.8 Hz, 1H), 3.69 (m, 1H), 3.86 (m, 2H), 5.08–5.20 (m, 2H), 5.26 (m, 1H), 5.71–5.88 (m, 1H), 6.51 (br t, J = 5.6 Hz, 1H), 7.10–7.29 ppm (m, 5H); ^{13}C NMR (125 MHz, $CDCl_3$): δ = 18.5, 26.6, 33.8, 35.1, 40.6, 42.2, 54.0, 67.1, 116.6, 126.2, 128.5, 128.6, 133.8, 141.2, 150.3, 166.4, 172.4 ppm; IR: ν = 2868–2918, 1769, 1734, 1703, 1533, 1339, 1136 cm^{-1}; MS (ESI): m/z (%): 345.18 (7) $[M + H]^+$, 367.16 (100) $[M + Na]^+$, 711.8 (6) $[2M + Na]^+$; HRMS-ESI: m/z $[M + H]^+$ calcd for $C_{19}H_{25}N_2O_4$: 345.18088, found: 345.18124.

4.5.3. 1-(Propyl-3-enamino)thiocarbonyl-(3S)-3-[(1R)-(4-phenylbutanoyloxy)ethyl]azetidin-2-one (**4d**)

Purification by flash chromatography (DCM/AcOEt 99:1) gave **4d** (48 mg, 89%) as a colourless oil: $[\alpha]_D$ = 0.31 (c = 0.48); Rf = 0.56 (cyclohexane/AcOEt 5:2); ^{1}H NMR (300 MHz, $CDCl_3$): δ = 1.35 (d,

J = 6.4 Hz, 3H), 1.92 (m, 2H), 2.31 (m, 2H), 2.62 (m, 2H), 3.33–3.43 (m, 1H), 3.71–3.79 (m, 1H), 3.88 (m, 1H), 4.12–4.34 (m, 3H), 5.14–5.37 (m, 2H), 5.78 (m, 1H), 7.12–7.33 (m, 5H), 8.38 ppm (br s, 1H); ^{13}C NMR (75 MHz, $CDCl_3$): δ = 18.5, 26.6, 33.7, 35.1, 43.8, 47.2, 52.3, 67.0, 117.9, 126.1, 128.5 (2C), 132.0, 141.2, 164.6, 172.4, 178.0 ppm; IR: ν = 2912–2932, 1755, 1734, 1533, 1339, 1321, 1132 cm^{-1}; MS (ESI): m/z (%): 361.16 (16) $[M + H]^+$, 383.14 (100) $[M + Na]^+$, 743.29 (6) $[2M + Na]^+$; HRMS-ESI: m/z $[M + H]^+$ calcd for $C_{19}H_{25}N_2O_3S$: 345.18088, found: 345.18124.

4.5.4. 1-(Propyl-3-sulfanyl)carbonyl-(3S)-3-[(1R)-(4-phenylbutanoyloxy)ethyl]azetidin-2-one (**4e**)

Purification by flash chromatography (DCM/AcOEt 99:1) gave **4d** (27 mg, 76%) as a colourless oil: $[\alpha]_D$ = 0.47 (c = 0.17); Rf = 0.50 (cyclohexane/AcOEt 5:2); ^{1}H NMR (300 MHz, $CDCl_3$): δ = 1.00 (t, J = 7.4 Hz, 3H), 1.35 (d, J = 6.4 Hz, 3H), 1.67 (m, 2H), 1.93 (m, 2H), 2.30 (m, 2H), 2.63 (m, 2H), 2.94 (m, 2H), 3.42 (m, 1H), 3.62 (dd, J = 3.6 Hz, J = 7.3 Hz, 1H), 3.75 (dd, J = 6.5 Hz, J = 7.2 Hz, 1H), 5.28 (m, 1H), 7.15–7.31 ppm (m, 5H); ^{13}C NMR (75 MHz, $CDCl_3$): δ = 13.4, 18.5, 23.0, 26.5, 31.2, 33.7, 35.1, 41.7, 54.0, 67.3, 126.1, 128.5, 128.6, 141.3, 163.4, 165.8, 172.4 ppm; IR: ν = 2925–2962, 1788, 1732, 1663, 1454, 1308, 1240, 1130 cm^{-1}; MS (ESI): m/z (%): 364.16 (4) $[M + H]^+$, 386.14 (100) $[M + Na]^+$; HRMS-ESI: m/z $[M + H]^+$ calcd for $C_{19}H_{26}NO_4S$: 364.15771, found: 364.15797.

4.6. General procedure for esterification with carboxylic acid (**5b–d** and **7a**)

To a stirred solution of alcohol precursor, DCC (1.1 equiv) and DMAP (0.1 equiv) in dry DCM (13 mL/mmol), at 20 °C, was added a solution of the suitable carboxylic acid (1.1 equiv) in dry dichloromethane (7 mL/mmol) under argon atmosphere. After stirring overnight, the mixture was cooled in an ice-bath for precipitation of urea, filtered and concentrated under vacuum. After purification by flash chromatography (DCM/EtOAc), a colourless oil was obtained in all cases.

4.6.1. 1-(Pent-4-enoyl)-(3S)-3-[(1R)-(2-(benzyloxy)acetoyloxy)ethyl]azetidin-2-one (**5a**)

Purification by flash chromatography (DCM/AcOEt 98:2) gave **5a** (78 mg, 89%) as a colourless oil: $[\alpha]_D$ = −0.15 (c = 0.52);Rf = 0.38 (chex/AcOEt 5:3); ^{1}H NMR (300 MHz, $CDCl_3$): δ = 1.39 (d, J = 6.4 Hz, 3H), 2.39 (m, 2H), 2.76 (m, 2H), 3.42 (m, 1H), 3.52 (dd, J = 3.7 Hz, J = 7.8 Hz, 1H), 3.66 (dd, J = 6.7 Hz, J = 7.8 Hz, 1H), 4.06 (s, 2H), 4.60 (s, 2H), 5.02 (m, 2H), 5.35 (m, 1H), 5.81 (m, 1H), 7.21–7.41 ppm (m, 5H); ^{13}C NMR (75 MHz, $CDCl_3$): δ = 18.4, 27.9, 35.9, 40.0, 53.5, 67.1, 68.2, 73.4, 115.9, 128.1, 128.2, 128.6, 136.4, 136.9, 164.1, 169.5, 170.3 ppm; IR: ν = 2849–2957, 1788, 1701, 1339, 1317, 1190, 1115 cm^{-1}; MS (ESI): m/z (%): 346.20 (4) $[M + H]^+$, 368.16 (100) $[M + Na]^+$; HRMS-ESI: m/z $[M + Na]^+$ calcd for $C_{19}H_{23}NO_5Na$: 368.1474, found: 368.1469.

4.6.2. 1-(Propyl-3-enoxy)carbonyl-(3S)-3-[(1R)-(2-(benzyloxy)acetoyloxy)ethyl]azetidin-2-one (**5b**)

Purification by flash chromatography (DCM/AcOEt 98:2) gave **5b** (31 mg, 58%) as a colourless oil: $[\alpha]_D$ = −0.45 (c = 1.27); Rf = 0.16 (chex/AcOEt 5:2); ^{1}H NMR (300 MHz, $CDCl_3$): δ = 1.38 (d, J = 6.4 Hz, 3H), 3.42 (m, 1H), 3.58 (dd, J = 3.6 Hz, J = 7.1 Hz, 1H), 3.70 (m, 1H), 4.06 (s, 2H), 4.59 (s, 2H), 4.68 (d, J = 5.7 Hz, 2H), 5.18–5.44 (m, 3H), 5.82–5.99 (m, 1H), 7.21–7.37 ppm (m, 5H); ^{13}C NMR (75 MHz, $CDCl_3$): δ = 18.2, 41.3, 54.2, 66.9, 67.1, 68.1, 73.3, 119.3, 127.9, 128.0, 128.4, 130.9, 136.8, 148.7, 163.2, 169.3 ppm; IR: ν = 2932, 1811, 1759, 1734, 1377, 1329, 1261, 1124 cm^{-1}; MS (ESI): m/z (%): 348.14 (2) $[M + H]^+$, 370.13 (100) $[M + Na]^+$; HRMS-ESI: m/z $[M + H]^+$ calcd for $C_{18}H_{22}NO_6$: 348.14416, found: 348.14460.

4.6.3. 1-(Propyl-3-enamino)carbonyl-(3S)-3-[(1R)-(2-(benzyloxy)acetoyloxy)ethyl]azetidin-2-one (**5c**)

Purification by flash chromatography (DCM/AcOEt 98:2) gave **5c** (35 mg, 93%) as a colourless oil: $[\alpha]_D$ = −0.36 (c = 1.27); Rf = 0.27 (chex/AcOEt 5:2); ^{1}H NMR (300 MHz, $CDCl_3$): δ = 1.38 (d, J = 6.3 Hz, 3H), 3.43 (m, 1H), 3.58 (dd, J = 3.0 Hz, J = 6.9 Hz, 1H), 3.72 (m, 1H), 3.89 (m, 2H), 4.06 (s, 2H), 4.60 (s, 2H), 5.10–5.23 (m, 2H), 5.35 (m, 1H), 5.76–5.88 (m, 1H), 6.52 (br s, 1H), 7.28–7.39 ppm (m, 5H); ^{13}C NMR (75 MHz, $CDCl_3$): δ = 18.4, 40.7, 42.3, 53.8, 67.1, 68.1, 73.5, 116.7, 128.2, 128.2, 128.7, 133.8, 137.0, 150.3, 166.1, 169.6 ppm; IR: ν = 2912, 1767, 1703, 1528, 1340, 1275, 1202, 1124 cm^{-1}; MS (ESI): m/z (%): 347.16 (26) $[M + H]^+$, 369.14 (100) $[M + Na]^+$; HRMS-ESI: m/z $[M + H]^+$ calcd for $C_{18}H_{23}N_2O_5$: 347.16015, found: 347.16032.

4.6.4. 1-(Propyl-3-enamino)thiocarbonyl-(3S)-3-[(1R)-(2-(benzyloxy)acetoyloxy)ethyl]azetidin-2-one (**5d**)

Purification by flash chromatography (DCM/AcOEt 98:2) gave **5d** (37 mg, 74%) as a colourless oil: $[\alpha]_D$ = 0.08 (c = 1.78); Rf = 0.43 (chex/AcOEt 5:2); ^{1}H NMR (300 MHz, $CDCl_3$): δ = 1.37 (d, J = 6.3 Hz, 3H), 3.37 (m, 1H), 3.71 (dd, J = 3.2 Hz, J = 7.5 Hz, 1H), 3.87 (m, 1H), 4.06 (s, 2H), 4.19–4.29 (m, 2H), 4.59 (s, 2H), 5.15–5.27 (m, 2H), 5.34 (m, 1H), 5.87 (m, 1H), 7.26–7.44 (m, 5H), 8.36 ppm (br s, 1H); ^{13}C NMR (75 MHz, $CDCl_3$): δ = 18.2, 43.7, 47.0, 52.0, 66.9, 67.8, 73.3, 117.8, 127.9, 128.0, 128.4, 131.8, 136.7, 164.0, 169.3, 177.8 ppm; IR: ν = 2920, 1755, 1531, 1339, 1244, 1196, 1122 cm^{-1}; MS (ESI): m/z (%): 363.14 (94) $[M + H]^+$, 385.12 (100) $[M + Na]^+$; HRMS-ESI: m/z $[M + H]^+$ calcd for $C_{18}H_{23}N_2O_4S$: 363.13730, found: 363.13710.

4.6.5. 1-(Pent-4-enoyl)-(3S)-3-[(1R)-(4-(pyridin-4-yl)butanoyl)ethyl]azetidin-2-one (**7a**)

Purification by flash chromatography (DCM/AcOEt 9:1) gave **7a** (45 mg, 64%) as a colourless oil: $[\alpha]_D$ = 0.10 (c = 0.50); Rf = 0.36 (DCM/MeOH 9:1); ^{1}H NMR (500 MHz, $CDCl_3$): δ = 1.32 (d, J = 6.4 Hz, 3H), 1.90 (m, 2H), 2.28 (t, J = 7.4 Hz, 2H), 2.35 (m, 2H), 2.60 (m, 2H), 2.73 (m, 2H), 3.39 (m, 1H), 3.50 (dd, J = 3.7 Hz, J = 7.7 Hz, 1H), 3.63 (dd, J = 6.8 Hz, J = 7.6 Hz, 1H), 4.93–5.06 (m, 2H), 5.25 (m, 1H), 5.77 (m, 1H), 7.07 (d, J = 6.0 Hz, 2H), 8.46 ppm (d, J = 6.0 Hz, 2H); ^{13}C NMR (125 MHz, $CDCl_3$): δ = 18.3, 25.3, 27.9, 33.4, 34.2, 35.8, 39.8, 53.5, 67.4, 115.9, 123.9, 136.3, 149.8, 150.2, 164.4, 170.3, 171.9 ppm; IR: ν = 2922, 1786, 1734, 1701, 1603, 1313, 1238, 1132 cm^{-1}; MS (ESI): m/z (%): 345.18 (100) $[M + H]^+$, 367.16 (80) $[M + Na]^+$; HRMS-ESI: m/z $[M + H]^+$ calcd for $C_{19}H_{25}N_2O_4$: 345.18088, found: 345.18088.

4.7. General procedure for coupling isocyanate with alcohol function (**6a–d**)

To a stirred solution of the alcohol precursor (1 equiv) in dry DCM (7 mL/mmol) at r.t., was dropwise added the phenethyl isocyanate (1.1 equiv) under argon atmosphere, and finally $Ti(OtBu)_4$ (0.1 equiv). After 1 h, the solution was quenched, at low temperature, with a saturated aqueous solution of NH_4Cl and diluted with DCM. The aqueous layers were several times extracted with DCM and the organic layers were combined, dried over $MgSO_4$, filtered and concentrated under vacuum. After purification by flash chromatography (cyclohexane/AcOEt), white solids (**6b** and **6d**) or colourless oils were obtained (**6a** and **6c**).

4.7.1. 1-(Pent-4-enoyl)-(3S)-3-[(1R)-((2-phenylethylamino)carbonyloxy)-ethyl]azetidin-2-one (**6a**)

Purification by flash chromatography (DCM/AcOEt 9:1) gave **6a** (61 mg, 81%) as a colourless oil: $[\alpha]_D$ = −0.19 (c = 0.77); Rf = 0.71 (AcOEt); ^{1}H NMR (500 MHz, $CDCl_3$): δ = 1.33 (d, J = 6.3 Hz, 3H), 2.29–2.48 (m, 2H), 2.79 (m, 4H), 3.25–3.46 (m, 4H), 3.62 (m, 1H), 4.74 (br s, 1H), 4.95–5.10 (m, 2H), 5.15 (m, 1H), 5.82 (m, 1H), 7.04–7.42 ppm (m, 5H); ^{13}C NMR (125 MHz, $CDCl_3$): δ = 18.7, 28.0, 35.8,

36.0, 40.0, 42.2, 53.8, 67.9, 115.9, 126.6, 128.7, 128.8, 136.5, 138.7, 155.2, 164.6, 170.4 ppm; IR: ν = 2922, 1786, 1699, 1529, 1379, 1315, 1240, 1196, 1134 cm^{-1}; MS (ESI): *m/z* (%): 345.18 (4) $[M + H]^+$, 367.16 (100) $[M + Na]^+$; HRMS-ESI: *m/z* $[M + H]^+$ calcd for $C_{19}H_{25}N_2O_4$: 345.18088, found: 345.18129.

4.7.2. 1-(Propyl-3-enoxy)carbonyl-(3S)-3-[(1R)-((2-phenylethylamino)carbonyloxy)-ethyl]-azetidin-2-one (**6b**)

Purification by flash chromatography (DCM/AcOEt 9:1) gave **6b** (22 mg, 64%) as a white solid: $[\alpha]_D = -0.51$ (*c* = 1.32); *Rf* = 0.78 (AcOEt); ^1H NMR (500 MHz, $CDCl_3$): δ = 1.35 (d, *J* = 6.3 Hz, 3H), 2.81 (t, *J* = 6.9 Hz, 2H), 3.36 (m, 1H), 3.43 (m, 2H), 3.58 (dd, *J* = 3.5 Hz, *J* = 6.9 Hz, 1H), 3.68 (m, 1H), 4.71 (m, 3H), 5.14 (m, 1H), 5.25–5.44 (m, 2H), 5.94 (m, 1H), 7.14–7.20 (m, 2H), 7.21–7.26 (m, 1H), 7.27–7.34 ppm (m, 2H); ^{13}C NMR (125 MHz, $CDCl_3$): δ = 18.7, 36.1, 41.6, 42.3, 54.8, 67.3, 68.0, 119.5, 126.7, 128.8, 128.9, 131.3, 138.7, 149.0, 155.3, 163.9 ppm; IR: ν = 2912–2932, 1807, 1717, 1705, 1518, 1379, 1327, 1259, 1128 cm^{-1}; MS (ESI): *m/z* (%): 347.16 (3) $[M + H]^+$, 369.14 (49) $[M + Na]^+$, 715.29 (100) $[2M + Na]^+$; HRMS-ESI: *m/z* $[M + H]^+$ calcd for $C_{18}H_{23}N_2O_5$: 347.16015, found: 347.16044.

4.7.3. 1-(Propyl-3-enamino)carbonyl-(3S)-3-[(1R)-((2-phenylethylamino)carbonyloxy)-ethyl]-azetidin-2-one (**6c**)

Purification by flash chromatography (DCM/AcOEt 9:1) gave **6c** (29 mg, 70%) as a colourless oil: $[\alpha]_D = -0.73$ (*c* = 1.17); *Rf* = 0.45 (chex/AcOEt 5:3); ^1H NMR (300 MHz, $CDCl_3$): δ = 1.33 (d, *J* = 6.4 Hz, 3H), 2.80 (t, *J* = 6.9 Hz, 2H), 3.34–3.47 (m, 3H), 3.56 (dd, *J* = 3.0 Hz, *J* = 6.8 Hz, 1H), 3.68 (m, 1H), 3.95 (m, 2H), 4.72 (br s, 1H), 5.03–5.27 (m, 3H), 5.71–5.93 (m, 1H), 6.56 (br s, 1H), 7.08–7.36 ppm (m, 5H); ^{13}C NMR (75 MHz, $CDCl_3$): δ = 18.7, 36.1, 40.7, 42.3 (2C), 54.2, 67.7, 116.7, 126.7, 128.8, 128.9, 133.8, 138.7, 150.4, 155.3, 166.7 ppm; IR: ν = 2980, 1765, 1699, 1645, 1531, 1497, 1454, 1337, 1248, 1136 cm^{-1}; MS (ESI): *m/z* (%): 346.18 (9) $[M + H]^+$, 368.16 (100) $[M + Na]^+$; HRMS-ESI: *m/z* $[M + H]^+$ calcd for $C_{18}H_{24}N_3O_4$: 346.17613, found: 346.17636.

4.7.4. 1-(Propyl-3-enamino)thiocarbonyl-(3S)-3-[(1R)-((2-phenylethylamino)carbonyloxy)-ethyl]-azetidin-2-one (**6d**)

Purification by flash chromatography (DCM/AcOEt 95:5) gave **6d** (56 mg, 84%) as a white solid: $[\alpha]_D = 0.25$ (*c* = 0.60); *Rf* = 0.35 (AcOEt); ^1H NMR (300 MHz, $CDCl_3$): δ = 1.33 (d, *J* = 6.4 Hz, 3H), 2.80 (t, *J* = 6.9 Hz, 2H), 3.26–3.36 (m, 1H), 3.37–3.48 (m, 2H), 3.72 (dd, *J* = 3.2 Hz, *J* = 7.4 Hz, 1H), 3.84 (m, 1H), 4.20–4.34 (m, 2H), 4.75 (br s 1H), 5.09–5.34 (m, 3H), 5.76–5.98 (m, 1H), 7.09–7.36 (m, 5H), 8.42 ppm (br s, 1H); ^{13}C NMR (75 MHz, $CDCl_3$): δ = 18.7, 36.0, 42.2, 43.8, 47.2, 52.5, 67.5, 117.9, 126.6, 128.7, 128.9, 132.0, 138.6, 155.2, 164.8, 178.1 ppm; IR: ν = 2976, 1749, 1715, 1697, 1524, 1497, 1337, 1242, 1130 cm^{-1}; MS (ESI): *m/z* (%): 362.15 (16) $[M + H]^+$, 384.13 (100) $[M + Na]^+$; HRMS-ESI: *m/z* $[M + H]^+$ calcd for $C_{18}H_{24}N_3O_3S$: 362.15329, found: 362.15359.

4.8. In vitro assays for human FAAH

Tubes containing the enzyme [27] (10 mM Tris–HCl, 1 mM EDTA, 0.1% (w/v) BSA, pH 7.4, 165 μL), test compounds in DMSO or DMSO alone for controls (10 μL) and [^{3}H]-AEA (50,000 dpm, 2 μM final concentration, 25 μL) were incubated at 37 °C for 10 min. Reactions were stopped by rapidly placing the tubes in ice and adding 400 μL of ice-cold chloroform/methanol (1:1 v/v) followed by vigorous mixing. Phases were separated by centrifugation at 850 *g*, and aliquots (200 μL) of the upper methanol/buffer phase were counted for radioactivity by liquid scintillation counting. In all experiments, tubes containing buffer only were used as control for chemical hydrolysis (blank) and this value was systematically subtracted. Using these conditions, URB-597 (**2**, Chart 1) inhibits *h*FAAH with an IC_{50} value of 40 nM.

4.9. In vitro assays for human MGL activity

Tubes containing purified enzyme [29] (10 mM Tris–HCl, 1 mM EDTA, 0.1% (w/v) BSA, pH 8.0, 165 μL), test compounds in DMSO or DMSO alone for controls (10 μL) and [^{3}H]-2-OG (50,000 dpm, 2 μM final concentration, 25 μL) were preincubated at 20 °C for 30 min and incubated at 37 °C for 10 min. Reactions were stopped by rapidly placing the tubes in ice and adding 400 μL of ice-cold chloroform/methanol (1:1 v/v) followed by vigorous mixing. Phases were separated by centrifugation at 850 *g*, and aliquots (200 μL) of the lower chloroform phase were counted for radioactivity by liquid scintillation counting. In all experiments, tubes containing buffer only were used as control for chemical hydrolysis (blank) and this value was systematically subtracted.

4.10. Reversibility studies

In a total volume of 15 μL, human FAAH (27.5 μg) and inhibitors (or DMSO for controls) at concentrations allowing inhibition of the enzyme before dilution and no inhibition after the 100-fold dilution, were preincubated during 1 h at room temperature. The mixtures were then diluted 100-fold by adding assay buffer. Immediately after, an aliquot (175 μL) was taken and [^{3}H]-AEA (50,000 dpm, 2 μM final concentration, 25 μL) was added. Two samples were taken at 30 and 90 min after the dilution too. Each aliquots was incubated at 37 °C for 30 min and reactions were stopped by rapidly placing the tubes in ice and adding 400 μL of ice-cold chloroform/methanol (1:1 v/v) followed by vigorous mixing. Phases were separated by centrifugation at 850 *g*, and aliquots (200 μL) of the upper methanol/buffer phase were counted for radioactivity by liquid scintillation counting. In all experiments, tubes containing buffer only were used as control for chemical hydrolysis (blank) and this value was systematically subtracted.

4.11. Docking studies

The crystal structure of humanized rat FAAH (PDB code: 3PPM) was used [36]. Docking of the inhibitors into the active site of FAAH was performed using the GOLD program [52]. GOLD is based on a genetic algorithm, performing docking of flexible ligands into proteins with partial flexibility in the neighbourhood of the active site. Default settings were used for the genetic algorithm parameters. Twenty solutions were generated and ranked by GOLD score. The GOLD fitness function is made up of four components: protein–ligand hydrogen bond energy, protein–ligand van der Waals energy, ligand internal van der Waals energy, and ligand torsional strain energy. The figures were produced using PyMOL [53].

Acknowledgement

The UCL (Université catholique de Louvain) and the F. R. S.-FNRS (Fonds de la Recherche Scientifique, Belgium) are gratefully acknowledged for financial support of this work (FRFC grant, no. 2.4.654.06 F). This work is partially supported by the Interuniversity Attraction Pole program (IAP P6/19 PROFUSA). J.M.-B. and C.M. are senior research associate of the Belgian F. R. S.-FNRS. The authors wish to thank Kaneka Corporation (Japan), in particular Dr. Claudio Salvagnini, for providing the starting azetidinone ((3*R*,4*R*)-3-[(*R*)-1′-(*tert*-butyldimethylsilyloxy)-ethyl]-4-acetoxy-2-azetidinone). Dr Geoffray Labar is acknowledged for the preparation of *h*FAAH, and Bouazza Es Saadi for technical assistance.

Appendix A. Supplementary material

Supplementary material associated with this article can be found, in the online version, at http://dx.doi.org/10.1016/j.ejmech.2012.11.035.

References

[1] M. Seierstad, J.G. Breitenbucher, Discovery and development of fatty acid amide hydrolase (FAAH) inhibitors, J. Med. Chem. 51 (2008) 7327–7343.
[2] S. Vandevoorde, Overview of the chemical families of fatty acid amide hydrolase and monoacylglycerol lipase inhibitors, Curr. Top. Med. Chem. 8 (2008) 247–267.
[3] M. Feledziak, D.M. Lambert, J. Marchand-Brynaert, G.G. Muccioli, Inhibitors of the endocannabinoid-degrading enzymes, or how to increase endocannabinoid's activity by preventing their hydrolysis, Recent Pat. CNS Drug Discov. 7 (2012) 49–70.
[4] A. Minkkila, S.M. Saario, T. Nevalainen, Discovery and development of endocannabinoid-hydrolyzing enzyme inhibitors, Curr. Top. Med. Chem. 10 (2010) 828–858.
[5] K. Otrubova, C. Ezzili, D.L. Boger, The discovery and development of inhibitors of fatty acid amide hydrolase (FAAH), Bioorg. Med. Chem. Lett. 21 (2011) 4674–4685.
[6] I.K. Khanna, C.W. Alexander, Fatty acid amide hydrolase inhibitors – progress and potential, CNS Neurol. Disord. Drug Targets 10 (2011) 545–558.
[7] D.L. Boger, H. Miyauchi, W. Du, C. Hardouin, R.A. Fecik, H. Cheng, I. Hwang, M.P. Hedrick, D. Leung, O. Acevedo, C.R.W. Guimaraes, W.L. Jorgensen, B.F. Cravatt, Discovery of a potent, selective, and efficacious class of reversible alpha-ketoheterocycle inhibitors of fatty acid amide hydrolase effective as analgesics, J. Med. Chem. 48 (2005) 1849–1856.
[8] D. Piomelli, G. Tarzia, A. Duranti, A. Tontini, M. Mor, T.R. Compton, O. Dasse, E.P. Monaghan, J.A. Parrott, D. Putman, Pharmacological profile of the selective FAAH inhibitor KDS-4103 (URB597), CNS Drug Rev. 12 (2006) 21–38.
[9] D.S. Johnson, C. Stiff, S.E. Lazerwith, S.R. Kesten, L.K. Fay, M. Morris, D. Beidler, M.B. Liimatta, S.E. Smith, D.T. Dudley, N. Sadagopan, S.N. Bhattachar, S.J. Kesten, T.K. Nomanbhoy, B.F. Cravatt, K. Ahn, Discovery of PF-04457845: a highly potent, orally bioavailable, and selective urea FAAH inhibitor, ACS Med. Chem. Lett. 2 (2010) 91–96.
[10] S.D. Roughley, H. Browne, A.T. Macias, K. Benwell, T. Brooks, J. D'Alessandro, Z. Daniels, S. Dugdale, G. Francis, B. Gibbons, T. Hart, T. Haymes, G. Kennett, S. Lightowler, N. Matassova, H. Mansell, A. Merrett, A. Misra, A. Padfield, R. Parsons, R. Pratt, A. Robertson, H. Simmonite, K. Tan, S.B. Walls, M. Wong, Fatty acid amide hydrolase inhibitors. 3: tetra-substituted azetidine ureas with in vivo activity, Bioorg. Med. Chem. Lett. 22 (2012) 901–906.
[11] M.J. Meyers, S.A. Long, M.J. Pelc, J.L. Wang, S.J. Bowen, B.A. Schweitzer, M.V. Wilcox, J. McDonald, S.E. Smith, S. Foltin, J. Rumsey, Y.-S. Yang, M.C. Walker, S. Kamtekar, D. Beidler, A. Thorarensen, Discovery of novel spirocyclic inhibitors of fatty acid amide hydrolase (FAAH). Part 2. Discovery of 7-azaspiro[3.5]nonane urea PF-04862853, an orally efficacious inhibitor of fatty acid amide hydrolase (FAAH) for pain, Bioorg. Med. Chem. Lett. 21 (2011) 6545–6553.
[12] K. Ahn, D.S. Johnson, M. Mileni, D. Beidler, J.Z. Long, M.K. McKinney, E. Weerapana, N. Sadagopan, M. Liimatta, S.E. Smith, S. Lazerwith, C. Stiff, S. Kamtekar, K. Bhattacharya, Y. Zhang, S. Swaney, K. Van Becelaere, R.C. Stevens, B.F. Cravatt, Discovery and characterization of a highly selective FAAH inhibitor that reduces inflammatory pain, Chem. Biol. 16 (2009) 411–420.
[13] E. de Lago, S. Petrosino, M. Valenti, E. Morera, S. Ortega-Gutierrez, J. Fernandez-Ruiz, V. Di Marzo, Effect of repeated systemic administration of selective inhibitors of endocannabinoid inactivation on rat brain endocannabinoid levels, Biochem. Pharmacol. 70 (2005) 446–452.
[14] F.A. Moreira, M. Grieb, B. Lutz, Central side-effects of therapies based on CB1 cannabinoid receptor agonists and antagonists: focus on anxiety and depression, Best Pract. Res. Clin. Endocrinol Metab. 23 (2009) 133–144.
[15] G. Gerra, A. Zaimovic, M.L. Gerra, R. Ciccocioppo, A. Cippitelli, G. Serpelloni, L. Somaini, Pharmacology and toxicology of Cannabis derivatives and endocannabinoid agonists, Recent Pat. CNS Drug Discov. 5 (2010) 46–52.
[16] J. Schlosburg, S. Kinsey, A. Lichtman, Targeting fatty acid amide hydrolase (FAAH) to treat pain and inflammation, AAPS J. 11 (2009) 39–44.
[17] K. Ahn, S.E. Smith, M.B. Liimatta, D. Beidler, N. Sadagopan, D.T. Dudley, T. Young, P. Wren, Y. Zhang, S. Swaney, K. Van Becelaere, J.L. Blankman, D.K. Nomura, S.N. Bhattachar, C. Stiff, T.K. Nomanbhoy, E. Weerapana, D.S. Johnson, B.F. Cravatt, Mechanistic and pharmacological characterization of PF-04457845: a highly potent and selective fatty acid amide hydrolase inhibitor that reduces inflammatory and noninflammatory pain, J. Pharmacol. Exp. Ther. 338 (2011) 114–124.
[18] L.J. Alvarez-Jaimes, J.A. Palmer, The role of endocannabinoids in pain modulation and the therapeutic potential of inhibiting their enzymatic degradation, Curr. Pharm. Biotechnol. 10 (2011) 1644–1659.
[19] C. Ezzili, M. Mileni, N. McGlinchey, J.Z. Long, S.G. Kinsey, D.G. Hochstatter, R.C. Stevens, A.H. Lichtman, B.F. Cravatt, E.J. Bilsky, D.L. Boger, Reversible competitive α-ketoheterocycle inhibitors of fatty acid amide hydrolase containing additional conformational constraints in the acyl side chain: orally active, long-acting analgesics, J. Med. Chem. 54 (2011) 2805–2822.
[20] J.A. Palmer, E.S. Higuera, L. Chang, S.R. Chaplan, Fatty acid amide hydrolase inhibition enhances the anti-allodynic actions of endocannabinoids in a model of acute pain adapted for the mouse, Neuroscience 154 (2008) 1554–1561.
[21] B.F. Cravatt, O. Prospero-Garcia, G. Siuzdak, N.B. Gilula, S.J. Henriksen, D.L. Boger, R.A. Lerner, Chemical characterization of a family of brain lipids that induce sleep, Science (New York, NY) 268 (1995) 1506–1509.
[22] S.G. Kinsey, S.T. O'Neal, J.Z. Long, B.F. Cravatt, A.H. Lichtman, Inhibition of endocannabinoid catabolic enzymes elicits anxiolytic-like effects in the marble burying assay, Pharmacol. Biochem. Behav. 98 (2011) 21–27.
[23] G.L. Li, H. Winter, R. Arends, G.W. Jay, V. Le, T. Young, J.P. Huggins, Assessment of the pharmacology and tolerability of PF-04457845, an irreversible inhibitor of fatty acid amide hydrolase-1, in healthy subjects, Br. J. Clin. Pharmacol. 73 (2012) 706–716.
[24] M. Feledziak, C. Michaux, A. Urbach, G. Labar, G.G. Muccioli, D.M. Lambert, J. Marchand-Brynaert, β-Lactams derived from a carbapenem chiron are selective inhibitors of human fatty acid amide hydrolase versus human monoacylglycerol lipase, J. Med. Chem. 52 (2009) 7054–7068.
[25] M. Feledziak, G.G. Muccioli, D.M. Lambert, J. Marchand-Brynaert, SAR and LC/MS studies of β-lactamic inhibitors of human fatty acid amide hydrolase (hFAAH): evidence of a nonhydrolytic process, J. Med. Chem. 54 (2011) 6812–6823.
[26] C. Spino, M.-A. Joly, C. Godbout, M. Arbour, Ti-catalyzed reactions of hindered isocyanates with alcohols, J. Org. Chem. 70 (2005) 6118–6121.
[27] G. Labar, F.V. Vliet, J. Wouters, D.M. Lambert, A MBP-FAAH fusion protein as a tool to produce human and rat fatty acid amide hydrolase: expression and pharmacological comparison, Amino Acids 34 (2008) 127–133.
[28] P. Ertl, B. Rohde, P. Selzer, Fast calculation of molecular polar surface area as a sum of fragment-based contributions and its application to the prediction of drug transport properties, J. Med. Chem. 43 (2000) 3714–3717.
[29] G. Labar, C. Bauvois, G.G. Muccioli, J. Wouters, D.M. Lambert, Disulfiram is an inhibitor of human purified monoacylglycerol lipase, the enzyme regulating 2-arachidonoylglycerol signaling, ChemBioChem 8 (2007) 1293–1297.
[30] D.L. Boger, H. Sato, A.E. Lerner, M.P. Hedrick, R.A. Fecik, H. Miyauchi, G.D. Wilkie, B.J. Austin, M.P. Patricelli, B.F. Cravatt, Exceptionally potent inhibitors of fatty acid amide hydrolase: the enzyme responsible for degradation of endogenous oleamide and anandamide, Proc. Natl. Acad. Sci. U.S.A. 97 (2000) 5044–5049.
[31] M. Mor, S. Rivara, A. Lodola, P.V. Plazzi, G. Tarzia, A. Duranti, A. Tontini, G. Piersanti, S. Kathuria, D. Piomelli, Cyclohexylcarbamic acid 3′- or 4′-substituted biphenyl-3-yl esters as fatty acid amide hydrolase inhibitors: synthesis, quantitative structure–activity relationships, and molecular modeling studies, J. Med. Chem. 47 (2004) 4998–5008.
[32] K. Ahn, D.S. Johnson, L.R. Fitzgerald, M. Liimatta, A. Arendse, T. Stevenson, E.T. Lund, R.A. Nugent, T.K. Nomanbhoy, J.P. Alexander, B.F. Cravatt, Novel mechanistic class of fatty acid amide hydrolase inhibitors with remarkable selectivity, Biochemistry 46 (2007) 13019–13030.
[33] M. Mileni, S. Kamtekar, D.C. Wood, T.E. Benson, B.F. Cravatt, R.C. Stevens, Crystal structure of fatty acid amide hydrolase bound to the carbamate inhibitor URB597: discovery of a deacylating water molecule and insight into enzyme inactivation, J. Mol. Biol. 400 (2010) 743–754.
[34] M. Mileni, J. Garfunkle, J.K. DeMartino, B.F. Cravatt, D.L. Boger, R.C. Stevens, Binding and inactivation mechanism of a humanized fatty acid amide hydrolase by α-ketoheterocycle inhibitors revealed from cocrystal structures, J. Am. Chem. Soc. 131 (2009) 10497–10506.
[35] M. Mileni, J. Garfunkle, C. Ezzili, F.S. Kimball, B.F. Cravatt, R.C. Stevens, D.L. Boger, X-ray crystallographic analysis of α-ketoheterocycle inhibitors bound to a humanized variant of fatty acid amide hydrolase, J. Med. Chem. 53 (2010) 230–240.
[36] M. Mileni, J. Garfunkle, C. Ezzili, B.F. Cravatt, R.C. Stevens, D.L. Boger, Fluoride-mediated capture of a noncovalent bound state of a reversible covalent enzyme inhibitor: X-ray crystallographic analysis of an exceptionally potent α-ketoheterocycle inhibitor of fatty acid amide hydrolase, J. Am. Chem. Soc. 133 (2011) 4092–4100.
[37] D.J. Gustin, Z. Ma, X. Min, Y. Li, C. Hedberg, C. Guimaraes, A.C. Porter, M. Lindstrom, D. Lester-Zeiner, G. Xu, T.J. Carlson, S. Xiao, C. Meleza, R. Connors, Z. Wang, F. Kayser, Identification of potent, noncovalent fatty acid amide hydrolase (FAAH) inhibitors, Bioorg. Med. Chem. Lett. 21 (2011) 2492–2496.
[38] X. Min, S.T. Thibault, A.C. Porter, D.J. Gustin, T.J. Carlson, H. Xu, M. Lindstrom, G. Xu, C. Uyeda, Z. Ma, Y. Li, F. Kayser, N.P.C. Walker, Z. Wang, Discovery and molecular basis of potent noncovalent inhibitors of fatty acid amide hydrolase (FAAH), Proc. Natl. Acad. Sci. U.S.A. 108 (2011) 7379–7384.
[39] L. Hedstrom, Serine protease mechanism and specificity, Chem. Rev. 102 (2002) 4501–4524.
[40] M. Lee, D. Hesek, M. Suvorov, W. Lee, S. Vakulenko, S. Mobashery, A mechanism-based inhibitor targeting the *D-D*-transpeptidase activity of bacterial penicillin-binding proteins, J. Am. Chem. Soc. 125 (2003) 16322–16326.
[41] J.-E. Hugonnet, J.S. Blanchard, Irreversible inhibition of the *Mycobacterium tuberculosis* β-lactamase by clavulanate, Biochemistry 46 (2007) 11998–12004.
[42] S. Vanwetswinkel, J. Fastrez, J. Marchand-Brynaert, Synthesis of new sulfonylamido-penicillanic acid sulfones inhibitors of beta-lactamases, J. Antibiot. 47 (1994) 1041–1051.
[43] W.B. Knight, A.L. Maycock, B.G. Green, B.M. Ashe, P. Gale, H. Weston, P.E. Finke, W.K. Hagmann, S.K. Shah, J.B. Doherty, Mechanism of inhibition of human leukocyte elastase by two cephalosporin derivatives, Biochemistry 31 (1992) 4980–4986.

[44] J.B. Doherty, B.M. Ashe, L.W. Argenbright, P.L. Barker, R.J. Bonney, G.O. Chandler, M.E. Dahlgren, C.P. Dorn, P.E. Finke, R.A. Firestone, D. Fletcher, W.K. Hagmann, R. Mumford, L. O'Grady, A.L. Maycock, J.M. Pisano, S.K. Shah, K.R. Thompson, M. Zimmerman, Cephalosporin antibiotics can be modified to inhibit human leukocyte elastase, Nature 322 (1986) 192–194.
[45] J. Mulchande, R.C. Guedes, W.-Y. Tsang, M.I. Page, R. Moreira, J. Iley, Azetidine-2,4-diones (4-oxo-β-lactams) as scaffolds for designing elastase inhibitors, J. Med. Chem. 51 (2008) 1783–1790.
[46] C. Beauve, G. Tjoens, R. Touillaux, J. Lamotte-Brasseur, J. Marchand-Brynaert, J. Fastrez, 1-Alkoxycarbonyl-3-bromoazetidin-2-ones as potential elastase inhibitors, Eur. J. Org. Chem. 1999 (1999) 1441–1447.
[47] M.I. Konaklieva, Beta-lactams as inhibitors of serine enzymes, Curr. Med. Chem. Anti-infect. Agents 1 (2002) 215–238.
[48] M.K. McKinney, B.F. Cravatt, Structure and function of fatty acid amide hydrolase, Annu. Rev. Biochem. 74 (2005) 411–432.
[49] J.P. Alexander, B.F. Cravatt, Mechanism of carbamate inactivation of FAAH: implications for the design of covalent inhibitors and in vivo functional probes for enzymes, Chem. Biol. 12 (2005) 1179–1187.
[50] M. Mileni, D.S. Johnson, Z. Wang, D.S. Everdeen, M. Liimatta, B. Pabst, K. Bhattacharya, R.A. Nugent, S. Kamtekar, B.F. Cravatt, K. Ahn, R.C. Stevens, Structure-guided inhibitor design for human FAAH by interspecies active site conversion, Proc. Natl. Acad. Sci. U.S.A. 105 (2008) 12820–12824.
[51] X. Wang, K. Sarris, K. Kage, D. Zhang, S.P. Brown, T. Kolasa, C. Surowy, O.F. El Kouhen, S.W. Muchmore, J.D. Brioni, A.O. Stewart, Synthesis and evaluation of benzothiazole-based analogues as novel, potent, and selective fatty acid amide hydrolase inhibitors, J. Med. Chem. 52 (2009) 170–180.
[52] G. Jones, P. Willett, R.C. Glen, A.R. Leach, R. Taylor, Development and validation of a genetic algorithm for flexible docking, J. Mol. Biol. 267 (1997) 727–748.
[53] W.L. De Lano, The PyMOL Molecular Graphics System, 0.99, DeLano Scientific, San Carlos, 2002.